Journal of Groundwater Science and Engineering 14(2026) 148–164

Journal homepage: http://gwse.iheg.org.cn

Research Article

Assessment of the natural background levels of ammonia nitrogen and chloride in alluvial fan groundwater using an improved pre-selection method: Implications for groundwater management

Chu Yu[1,2], Ze-peng Zhang[1,2*], Yi-long Zhang[1,2], Heng-xin Zhang[1,2], Xiao-han Li[1,2]

[1] *Institute of Hydrogeology and Environmental Geology*, *Chinese Academy of Geological Sciences*, *Shijiazhuang* 050061, *China*.
[2] *Key Laboratory of Groundwater Science and Engineering*, *Ministry of Natural Resources*, *Shijiazhuang* 050061, *China*.

Abstract: Natural Background Levels (NBLs) play a pivotal role in groundwater management. Ammonia nitrogen exceeding national standards is a significant concern in the alluvial fan area of Tuzuoqi, Hohhot, Inner Mongolia. The commonly used pre-selection method relies on empirical judgment with predefined pollution thresholds, making it highly subjective and less adaptable. In this study, an improved pre-selection approach was used to assess the NBLs of ammonia nitrogen and chlorides in the study area, complemented by pollution indices to evaluate the extent and scope of contamination. The improved method first employed Hierarchical Clustering Analysis (HCA) to identify characteristic pollution indicators, including NH_4^+, Cl^-, TDS, Ca^{2+}, Na^+, NO_3^-, and Chlorinated HydroCarbons (CHCs). Subsequently, the contamination levels of these indicators were analyzed to establish pollution thresholds and remove contaminated samples, thereby completing the pre-selection of original samples. The pre-selection criteria for the study area were: For ammonia nitrogen, NH_4^+-N > 0.5 mg/L combined with Cl^- > 250 mg/L; for chloride, Cl^- > 250 mg/L and Cl^- > 100 mg/L with simultaneous detection of CHCs. Pre-selected samples were further analyzed using Grubbs' test to identify NBLs samples. The validity of the NBLs samples was confirmed through significance tests based on historical data. The 95th percentile of the NBLs samples was used to calculate a unified NBLs for pollution indices. The results indicate that ammonia nitrogen contamination is concentrated in the central-southern part of the industrial park, with a limited spatial extent and severe pollution near pollution sources. The exceedances of ammonia nitrogen in water source wells are due to high NBLs, which are attributed to organic-rich alluvial-lacustrine interbedded deposits. Chloride pollution has spread from the central-southern to the northern areas, causing slight contamination in some wells over a broader region. Compared to other alluvial fans, elevated chloride NBLs are related to the high content of water-soluble salts in the lacustrine sediments within the strata. This study validates the effectiveness of the improved preselection method in determining groundwater NBLs and emphasizes the role of NBLs in identifying sources and contamination levels of exceeding components.

Keywords: NBLs; Preselection method; Ammonia nitrogen; Chlorine; Hohhot Basin; Groundwater contamination

Received: 25 Mar 2025/ Accepted: 27 Oct 2025/ Published: 30 Apr 2026

*Corresponding author: Ze-peng Zhang, *E-mail address*: 358288386@qq.com

DOI: 10.26599/JGSE.2026.9280076

Yu C, Zhang ZP, Zhang YL, et al. 2026. Assessment of the natural background levels of ammonia nitrogen and chloride in alluvial fan groundwater using an improved pre-selection method: Implications for groundwater management. Journal of Groundwater Science and Engineering, 14(2): 148-164.

Introduction

Natural Background Levels (NBLs) serve as essential benchmarks for establishing contamination remediation objectives and for assessing the anthropogenic influence on the natural chemical constituents of groundwater (Lan et al. 2024; Allia and Lalaoui, 2024). Evaluating NBLs is a crucial initial step in assessing groundwater contamination and formulating regulatory guidelines. The

European Groundwater Directive (2006/118/EC) (European, 2006) describes NBLs as concentrations of substances in groundwater with little to no anthropogenic influence, a definition widely accepted in the field (Reimann and Garrett, 2005; Panno et al. 2006; Nisi et al. 2016). Given the inherent heterogeneity and anisotropy of aquifers, NBLs vary spatially even within the same hydrogeologic unit, indicating that they represent not singular values but a range (Reimann and Garrett, 2005; Guo et al. 2010).

Groundwater NBLs evaluation typically involves two main approaches: The use of mathematical statistics (Parrone et al. 2019) and the pre-selection method (Bulut et al. 2020; Serianz et al. 2020). In the mathematical statistics, various statistical metrics are applied to define NBLs based on data distribution patterns. Commonly, the formulas MEAN±2·SD (mean plus or minus two times the standard deviation), along with MED±2·MAD and [Q25-1.5·IQR, Q75+1.5·IQR] (Biddau et al. 2017; Gao et al. 2020) is used for data following normal or log-normal distributions, while [Q2.5, Q97.5] is more appropriate for skewed data distributions, each method having its own advantages and limitations (Bondu et al. 2022). Relying solely on mathematical statistics can overlook the complex interactions among hydrochemical components and the intrinsic evolutionary dynamics of groundwater chemistry, potentially leading to NBLs that do not accurately reflect natural conditions (He et al. 2022).

The pre-selection method aims to identify pristine groundwater samples, commonly referred to as Pre-Selected (PS) samples, with minimal anthropogenic interference by filtering out contaminated samples using predefined thresholds for certain indicators. Common contaminant indicators employed in this method include dissolved oxygen, NH_4^+, NO_3^-, Cl^-, and SO_4^{2-} (Hinsby et al. 2008; Ducci et al. 2016; Parrone et al. 2019; Chen et al. 2022). However, this method may ever overestimate or underestimate NBLs (Huang et al. 2022) because the thresholds for these indicators are largely based on empirical values that might not accurately reflect local hydrogeochemical conditions. Moreover, due to the variety of contamination sources and the diversity of groundwater contaminants, these common indicators do not always successfully identify contaminated samples (De Caro et al. 2017; Serianz et al. 2020). For example, while NO_3 may effectively pinpoint samples impacted by agricultural activities and domestic life, it might not reliably screen out samples influenced by industrial activities. In certain specific conditions, these indicators may not provide any useful information. For example, NH_4 may not be a reliable indicator in aquifers rich in organic matter (Molinari et al. 2012).

In recent years, numerous researchers have explored NBLs determination by integrating various methodologies (Ducci et al. 2016; Bi et al. 2022; Bondu et al. 2022; Khadra et al. 2022). They establish thresholds for one or more key contamination markers through empirical or geochemical analyses. Utilizing these thresholds, they filter samples showing negligible or no anthropogenic interference, thereby finalizing the pre-selection of pristine groundwater samples. Subsequent statistical analyses and tests on the PS dataset involve selecting appropriate statistical metrics to define NBLs based on the data's statistical properties. These investigations indicate that combining the pre-selection and statistical approaches can significantly improve the accuracy of NBLs estimation.

The study area is situated on an alluvial-proluvial fan, with groundwater serving as the main source for daily and industrial needs of the local population. Over the past two decades, rapid industrial development has been accompanied by increased groundwater extraction. Recent studies have shown that the NH_4^+-N concentration in groundwater of water source wells can reach as high as 5.15 mg/L, far exceeding the national Class III water quality standard of 0.5 mg/L, with an annual increase rate of 0.17 mg/L (Liu et al. 2023). This poses a threat to regional water supply safety. Local environmental authorities are therefore urgently interested in determining whether such elevated ammonia nitrogen levels are related to industrial activities and to what extent. Establishing groundwater NBLs is essential for understanding the causes of exceedances and for setting realistic remediation targets.

In this study, an improved pre-selection method was employed to evaluate the NBLs of ammonia nitrogen and chloride in the study area, as ammonia nitrogen in water sources has attracted particular attention, while chloride is a major hydrogeochemical component and a common indicator in hydrogeochemical analyses. Unlike traditional approaches that rely on empirical thresholds for pre-selection, this method involves: (1) Selecting characteristic pollution indicators based on Hierarchical Cluster Analysis (HCA), including ammonia nitrogen and seven other parameters; and (2) delineating pollution thresholds based on the concentration features of these indicators. Due to their differing hydrogeochemical features, pollution sources, and levels, ammonia nitrogen and

chloride have distinct pollution criteria and standards. The pre-selected samples were analyzed using Grubbs' test to obtain the NBLs dataset. This dataset was then validated using historical hydrochemical data and statistical methods. Finally, a preliminary assessment of groundwater pollution was conducted based on pollution indices calculated from the unified NBLs.

1 Study area

1.1 Geographical conditions

As depicted in Fig. 1, the study area is located in Tuzuoqi, Hohhot, Inner Mongolia, China, bordered by a low-to-mid mountain range to the north and surrounded by alluvial-proluvial plains on the remaining sides, encompassing an area of approximately 181 km^2. The study area experiences a medium-temperate continental monsoon climate, characterized by aridity, limited rainfall, and significant evaporation rates. The average annual temperature stands at 7.2°C, with peak and minimum monthly average temperatures typically occurring in July and December, respectively. The study area receives an average annual rainfall of 388.2 mm, sees an average annual evaporation rate of 3,259.8 mm, maintains an average annual relative humidity of around 53.6%, and enjoys an average annual sunshine duration of approximately 2,883.5 hours. The predominant soil types are meadow soil and gray cinnamon soil. Although the study area lacks permanent surface water bodies, three seasonal streams can be found in the northern mountainous region.

1.2 Geological and hydrogeological conditions

Throughout the Cenozoic, the Hohhot region underwent significant geological movements, characterized by a southward descent and northward rise, driven by NW-SE-oriented extensional forces. This resulted in the formation of the Hohhot faulted basin. The basin is notable for its exceptionally thick strata ranging from the Paleogene Eocene to the Quaternary, with the study area situated at the basin's subsidence center. Since the Middle Pleistocene, this subsidence center has predominantly accumulated lacustrine sediments, leading to the development of a stable and widespread silty clay layer. This layer acts as an confining layer between the shallow and deep groundwater aquifers (Zhang et al. 2017). Since the Late Pleistocene, the area's geological composition has been predominantly alluvial-proluvial sediments. Unique climatic conditions have facilitated periodic expansions of the lake surface, resulting in the formation of alluvial-lacustrine interbedded deposits in the shallow subsurface. The aquifer contains high content of clay sediments and organic matter (Liu et al. 2023). Notably, multiple silty sediment layers have been identified up to depths of around 150 m in boreholes LS3, LS2, and TK31, as illustrated in Fig. 1.

In the study area, the apex of the alluvial-proluvial fan is marked by a discontinuous aquiclude, and an aquifer primarily consisting of sand and gravel layers that house phreatic water, with groundwater level depths typically found at 60 m to 70 m. Progressing from the fan's center to its periphery, a silty clay layer is consistently present, and aquifers are composed of gravel-bearing coarse sands, fine sands, and silty sands, where the groundwater level depths become progressively shallower. The superficial aquifer, situated above the clay layer, generally extends down to depths between 60 m to 80 m, with groundwater level depths varying from 30 m to 50 m. Conversely, the deeper confined aquifer beneath the clay layer starts at depths of roughly 150 m to 220 m and has a thickness often exceeding 100 m. Due to the significant depth of the confined aquifer, water extraction in the study area predominantly targets the shallower aquifer, with extraction depths usually ranging from 80 m to 150 m. The centralized water supply, positioned atop the fan as shown in Fig. 1, is supported by 12 source wells. The study area's groundwater primarily receives replenishment from the subterranean flow of adjacent mountain valleys, ensuring the aquifers' ample water supply, with individual well yields often surpassing 5,000 cubic meters per day. The general groundwater flow direction is from northeast to southwest, with hydraulic gradients spanning from 0.0006 to 0.0035. Intensive extraction from these source wells has led to the formation of a localized depression cone within the water source zone, causing groundwater to flow from the south towards the north (Liu et al. 2023).

1.3 Land use conditions

Mining and residential land, as well as agricultural land, constituted the main land use types in the study area, accounting for 27.92% and 39.46% of the area in 2020. Grassland accounted for 21.65%, forest land accounted for 1.97%, water area

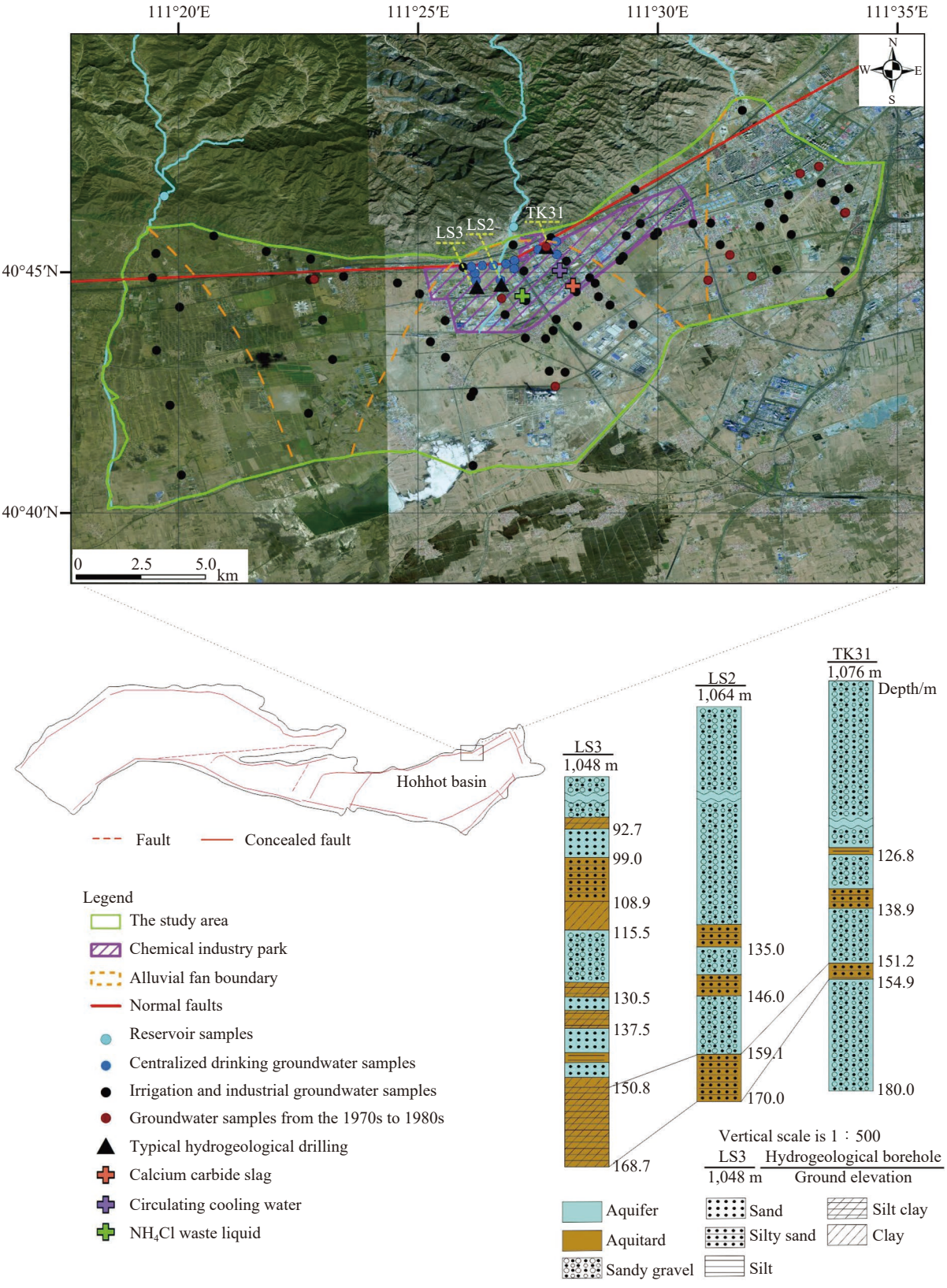

Fig. 1 The geographic position and fault structure diagram (lower left) of the study area

Notes: The distributions of surface water and groundwater sampling sites, potential contamination sources, typical hydrogeological boreholes, and preindustrial groundwater samples (upper), and lithological structures of strata in typical hydrogeological boreholes (lower).

accounted for 0.68%, and unused land accounted for 8.32%. The north-central part of the area features a national industrial park covering 16.5 km^2, accounting for 9% of the study area. Estab-

lished in 2003, it has experienced rapid industrial growth. From 2000 to 2020, the area of mining and residential land within the park increased from 1.42% to 84.25%.

1.4 Potential contamination sources

The industrial park hosts sixty-nine enterprises, with chemical manufacturing and dairy product processing being the predominant industries. The environmental impact assessments have identified PolyVinyl Chloride (PVC) and rare earth metal chemical plants, located in the park's southwest, as major sources of contamination (Fig. 1). Three key potential contamination sources have been recognized: The ammonium chloride (NH_4Cl) waste liquid generated by various production stages within the rare earth metal chemical plant, the recirculating cooling water pool and openly stored carbide slags at the PVC chemical plant.

2 Materials and methodology

2.1 Sampling and chemical analysis

In July 2021 and July 2022, samples were collected within the study area, with additional samples obtained in November 2021 and May 2022 as supplements. A total of 76 groundwater samples, including 12 from groundwater source wells, were analyzed for 12 parameters: NH_4^+-N, NO_3^--N, NO_2^--N, TDS, SO_4^{2-}, Cl^-, Ca^{2+}, Na^+, Fe, Mn, COD, and Br^-. A subset of these samples was also tested for 13 types of Chlorinated HydroCarbons (CHCs), such as trichloromethane (chloroform), carbon tetrachloride, 1,1-dichloroethane, dichloromethane, 1,2-dichloroethane, 1,1,1-trichloroethane, 1,1,2-trichloroethane, 1,2-dichloropropane, vinyl chloride, 1,1-dichloroethene, 1,2-dichloroethene, trichloroethene, and tetrachloroethene. Additionally, samples of calcium carbide slags and recirculating cooling water were collected to identify the characteristic contaminants of potential contamination sources. In the lab, a soil column leaching experiment was performed on the slag samples to examine the overall chemical makeup of the leachate, with the procedure outlined in Text S1. Due to the absence of NH_4Cl waste liquid samples, their analytical data were obtained from the existing environmental impact assessment report. Furthermore, two surface water samples were taken from a mountainous reservoir to characterize the hydrochemical profile of pristine groundwater.

The analytical methods included using an ultraviolet spectrophotometer (UV-2550, JPN) for NH_4^+-N and NO_2^--N measurements, a portable multiparameter water quality analyzer (Multi 3630, WTW, Germany) for TDS, an ion chromatograph (ICS-1500, Thermo Fisher Scientific, USA) for NO_3^--N, SO_4^{2-}, Cl^-, and Br^-, an inductively coupled plasma spectrometer (iCAP 6300, Thermo Fisher Scientific, USA) for Ca^{2+}, Na^+, Fe, and Mn, the acidic potassium permanganate method for COD, and a purge and trap concentrator combined with a gas chromatograph-mass spectrometer (GCMS-QP 2010 plus, JPN) for CHC analysis.

2.2 Data analysis and mapping

The investigation into the factors driving groundwater chemistry utilized Principal Component Analysis (PCA). Hierarchical cluster analysis, leveraging squared Euclidean distance and Ward's method, assessed the similarity between ammonia nitrogen and other potential characteristic pollution indicators within groundwater samples, thereby identifying key pollution indicators. Mahalanobis distance-based HCA with Ward's method was further applied to validate the identification of contaminated samples. Prior to statistical analysis, all data underwent standardization via the Z-score technique to mitigate the influence of the differences in data scales on the analysis outcomes. The tools employed for mapping included ArcGIS 10.8, OriginPro 2021, and SPSS 27.0.

2.3 NBLs evaluation

Step I involved the selection of characteristic pollution indicators through HCA, considering 11 parameters such as NO_3^--N, NO_2^--N, TDS, Cl^-, Ca^{2+}, Na^+, Fe, Mn, COD, Cl/Br, and CHCs. The selection adhered to four criteria: (1) Initially, direct reaction products of NH_4^+-N, such as NO_3^--N and NO_2^--N, were chosen; (2) Indicators representing potential contamination sources, such as TDS, Cl^-, Ca^{2+}, Na^+, and CHCs, were selected (Table S3); (3) Indicators reflecting aquifer oxidation-reduction conditions and concentrations of reducing substances, such as Fe, Mn, and COD, were considered (Wendland et al. 2008; Ducci et al. 2016; Bondu et al. 2022); (4) Lastly, the Cl/Br ratio, a common measure of anthropogenic influence, was selected.

Indicators grouped with NH_4^+-N in the dendrogram from cluster analysis were identified as char-

acteristic pollution indicators.

Step II focused on selecting contaminated groundwater samples based on NH_4^+-N, Cl^-, and other characteristic pollution indicators' concentration profiles, and pre-selecting the remaining groundwater samples. Initially, NH_4^+-N vs. Cl^- concentration plots were created for groundwater, surface water (from a mountainous reservoir), and potential contamination sources within the study area. Subsequently, the concentration profiles of other characteristic pollution indicators were integrated into these plots. Zones exhibiting high pollution indicator values were outlined, and thresholds for NH_4^+-N and Cl^- concentrations in groundwater were established. Samples within these defined thresholds were classified as contaminated and removed, with the rest included in the PS dataset (Huang et al. 2022). Validation of the identified contaminated samples based on the results of HCA of the samples.

Step III involved using Grubbs' test to remove outliers from the PS dataset, followed by selecting appropriate statistical metrics for NBLs characterization. At a designated significance level (α=0.01), outliers for specific chemical components were eliminated based on Grubbs' test outcomes (Analytical Methods Committee, 2015), which is particularly suitable for small sample sizes (Gao et al. 2020). The test flagged contaminated samples, which were then removed, leaving the remaining samples to represent background levels, which were designated as the NBLs dataset. Normality tests were performed on the NBLs dataset. For normally distributed data, the maximum value was used as the NBLs; for non-normal data, the 95th percentile was adopted to define the NBLs (Parrone et al. 2019; Bi et al. 2022; Huang et al. 2022).

Step IV involved conducting one-sample t-tests to evaluate whether differences between historical groundwater samples and the original and NBLs dataset were statistically significant. This process validated the appropriateness of the NBLs dataset and the assessment method, thus ensuring the reliability of subsequent assessments.

2.4 Pollution indices

The pollution index was used to evaluate the groundwater contamination degree by comparing the concentration of a chemical component, with the NBLs subtracted, to the national standard threshold. This index effectively reflects the anthropogenic influence and the extent to which the concentration of the component exceeds the Class III water quality standard. The equation for calculating the pollution index is as follows (MEEC, 2021):

$$P_i = (C_i - C_{NBLs}) / C_{III} \quad (1)$$

Where: P_i denotes the pollution index of inorganic component i in a sample; C_i is the test result of component i; C_{NBLs} is the NBLs of component i, and C_{III} is the Class III water standard threshold specified in GB/T 14848–2017, which is primarily applicable to centralized drinking water sources, as well as industrial and agricultural water (GAQS and IQPRC, 2017).

The pollution index classification criteria are as follows: (0, 0.2] for mild contamination, (0.2, 0.6] for moderate contamination, (0.6, 1.0] for heavy contamination, (1.0, 1.5] for severe contamination, and > 1.5 for extremely severe contamination.

3 Results and discussion

3.1 Chemical parameters and controlling factors of groundwater

3.1.1 General chemical parameters

The analytical results for the 12 chemical parameters are summarized in Table S1 and Fig. 2a and Fig. 2b. The detection rates of NH_4^+-N in non-groundwater source wells and groundwater source wells were 52% and 83%, respectively. According to the national Class III groundwater quality standard, NH_4^+-N had the highest exceedance rate in non-groundwater source wells, at 33%, with a maximum concentration of 529.32 mg/L. The exceedance rates followed the order: NH_4^+-N (33%) > Fe (23%) = Mn (23%) > COD (17%) > Cl^-(13%) > TDS (11%) > NO_2^--N (10%) = Na^+(10%) > NO_3^--N (8%) > SO_4^{2-} (3%). The coefficient of variation (CV) reflects the degree of variability of in the hydrogeochemical environment by quantifying the data dispersion. A high CV often suggests that the groundwater environment is strongly influenced by anthropogenic factors (Chen et al. 2022; Zhou et al. 2025). The CV of NH_4^+-N in non-groundwater source wells was as high as 7.01, and those of other components ranged from 0.71–2.41, implying that NH_4^+-N may be heavily affected by human activities.

In groundwater source wells, the maximum NH_4^+-N concentration was 5.15 mg/L, with an average of 1.68 mg/L, and an exceedance rate of 83%. Other parameters exceeding standards included NO_2^--N, Fe, Mn, and COD, with NO_2^--N

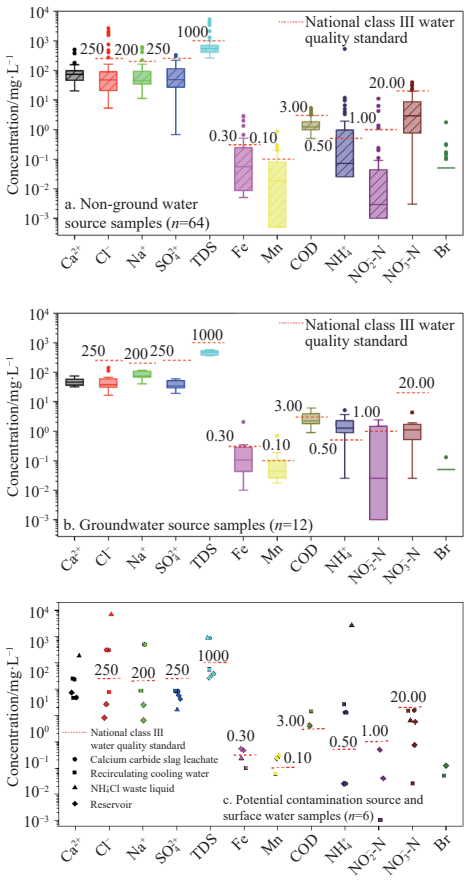

Fig. 2 Box plots showing the distribution of general chemical parameters in groundwater, surface water, and potential pollution source samples, compared with the national Class III groundwater quality standards

exhibiting a 33% exceedance rate, while the others had rates of 25%. The CV of NH_4^+-N in groundwater source wells was 0.89, much lower than that of non-groundwater source wells, and the CV of other parameters ranged from 0.17–1.93. This signifies that the groundwater source wells were only slightly impacted by anthropogenic activities, and the high NH_4^+-N concentrations are likely of geological origin.

Table S2 and Fig. 2c present the analytical findings for reservoir water and potential contamination sources. The surface water from the mountainous area serves as a significant contributor to groundwater recharge in the study area, with its hydrochemical profile reflecting the initial stages of water-rock interaction. The reservoir water sample showed lower TDS and reduced concentrations of SO_4^{2-}, Cl^-, Na^+, NO_3^--N, and NO_2^--N compared to the drinking water standards set nationally, with NH_4^+-N being undetectable. The potential contamination sources displayed distinct contamination signatures. The leachate from calcium carbide slags at the PVC chemical plant exhibited elevated TDS and high concentrations of Cl^-, Na^+, and NH_4^+-N, exceeding the national drinking water standards by factors of 8 to 25. The recirculating cooling water sample contained a high NH_4^+-N concentration and COD, surpassing standard thresholds by approximately 50 and 5 times, respectively, yet had low TDS and minimal Cl^- and Na^+ concentrations when compared to national standards. The NH_4Cl waste liquid from the rare earth metal chemical plant presented extremely high Cl^-, NH_4^+-N, and Ca^{2+} concentrations, with Cl^- and NH_4^+-N exceeding the national standards by hundreds to tens of thousands of times. Meanwhile, Fe, Mn, NO_3^--N, and NO_2^--N concentrations in all three potential contamination sources remained below the national drinking water thresholds.

3.1.2 CHCs

CHCs, prevalent organic contaminants in the resin manufacturing sector (Lu et al. 2023), are considered significant organic contaminants in the study area's groundwater. Their concentrations indicate the impact of chemical production activities on groundwater quality (Ducci et al. 2016; De Caro et al. 2017). Out of 13 CHCs tested, nine were detected (Table S3), with their detection frequencies listed as follows: Tetrachloroethylene (37%) > 1,2-dichloroethylene, trichloroethylene, and 1,1,2-trichloroethane (all at 34%) > 1,1-dichloroethane (31%) > 1,2-dichloroethane and chlorethylene (both at 29%) > 1,1-dichloroethylene and chloroform (both at 17%). The samples containing CHCs primarily originated from the industrial park's central and southern zones (Fig. S1), with total CHC concentrations spanning from 1.5 μg/L to 10,563.8 μg/L (mean: 2,491.9 μg/L). Among these, chloroform exhibited the highest mean concentration at 2,048.1 μg/L, reaching up to 9,010.0 μg/L in specific samples. The reservoir water sample contained no detectable CHCs. Of the identified potential contamination sources, only the PVC chemical plant's recirculating cooling water sample tested positive for CHCs, registering a total concentration of 160.4 μg/L (Table S2).

3.1.3 Analysis of controlling factors

PCA is widely utilized in hydrogeochemical studies to uncover hidden insights within complex data by reducing the dimensionality of the dataset by identifying key variables (Ahmadi et al. 2018). Br^- was excluded from further analysis due to its low detection rate of only 20% across samples. Employing the Kaiser-Harris criterion, three principal components (PC 1, PC 2, and PC 3), each

with eigenvalues exceeding 1, were identified, cumulatively explaining 79.1% of the variance (Table 1).

PC 1, contributing 48.8% to the total variance, showed strong positive associations with TDS (0.43), Cl^- (0.42), Ca^{2+} (0.39), Na^+ (0.39), NO_3^--N (0.35), SO_4^{2-} (0.33), and NH_4^+-N (0.30). Notably, TDS, Cl^-, Na^+, Ca^{2+}, and NH_4^+-N are characteristic pollution indicators of industrial contamination sources within the industrial park, suggesting that PC 1 primarily reflects industrial impacts on groundwater.

PC 2, representing 16.5% of the variance, had significant positive correlations with COD (0.61), NO_2^--N (0.47), Fe (0.44), and Mn (0.38). Given the high organic matter content in the alluvial-lacustrine sedimentary strata of the study area, the mineralization of organic matter can shift the groundwater to a reducing state. In such conditions, Fe and Mn oxides in sediments are reduced and leached into the groundwater, raising Fe and Mn concentrations, often correlating positively with COD (Xiong et al. 2022). Thus, PC 2 likely represents the organic matter mineralization in aquifers.

PC 3, explaining 13.8% of the variance, showed strong positive correlations with NO_2^--N (0.49), COD (0.36), and NH_4^+-N (0.21), and negative correlations with Mn (−0.57) and Fe (−0.48). NO_2^--N is an intermediate in NH_4^+-N nitrification. In aerobic conditions, the conversion of ionic Fe and Mn into oxides, which can adsorb NH_4^+-N, reduces ammonia nitrogen concentrations in groundwater (Zhang et al. 2020), suggesting PC 3 represents ammonia nitrogen denitrification.

Table 1 PCA-derived factor profile as the extraction criterion

Species	PC 1	PC 2	PC 3
TDS	0.43	0.05	0.04
SO_4^{2-}	0.33	−0.09	−0.08
Cl^-	0.42	0.03	0.08
Na^+	0.39	0.17	−0.08
Ca^{2+}	0.39	−0.06	0.04
Fe	0.03	0.44	−0.48
Mn	0.09	0.38	−0.57
COD	0.00	0.61	0.36
NH_4^+-N	0.30	0.03	0.21
NO_2^--N	−0.08	0.47	0.49
NO_3^--N	0.35	−0.19	0.10
Eigenvalue	5.37	1.81	1.51
Percentage of Variance	48.8%	16.5%	13.8%

Overall, PCs 2 and 3 depict the nitrogen cycle in aquifers under natural conditions. In summary, the results indicate that groundwater ammonia nitrogen is influenced by both industrial activities and natural processes, a finding supported by nitrogen isotope analysis (Liu et al. 2023).

Furthermore, the relationships among specific components were analyzed to elucidate hydrochemical controlling factors. The Na^+/Cl^- ratio is a useful indicator for identifying the predominant factors affecting hydrochemical characteristics and for determining the primary mineral sources of Na^+ and Cl^- in water-rock interactions (Magaritz et al. 1981; Xiao et al. 2016). In this study, the majority of groundwater samples plotted above the line representing a 1:1 molar concentration ratio of Na^+/Cl^- (Fig. 3a), indicating that the concentrations of Na^+ and Cl^- were mainly controlled by the dissolution of aluminosilicate minerals or cation exchange. However, some samples exhibited exceptionally high Cl^- concentrations, surpassing 10 mmol/L, suggesting a substantial anthropogenic contribution.

CHCs are characteristic pollutants in the recirculating cooling water of the PVC plant (as discussed in Section 4.1.2). The F-test for the linear regression between CHCs and Cl^- showed a p-value less than 0.05, indicating a significant influence of CHCs on Cl^- at the 5% significance level (Fig. 3b). This result suggests that the Cl^- concentrations at some sampling points are influenced by recirculating cooling water, including two groundwater source wells. The Cl^- levels in these two wells (3.16 mmol/L and 3.97 mmol/L) are markedly higher than those in other source wells (0.56–1.88 mmol/L), indicating that industrial activities have already impacted these water sources.

The relationship between Cl^- and NH_4^+-N is crucial in identifying contaminated groundwater. Given its conservative chemical behavior, Cl^- displays varied concentrations across natural fluids, solids, and diverse contamination sources. Elevated Cl^- concentrations are commonly indicative of groundwater influenced by human activities (Davis et al. 1998; Du et al. 2017). Under natural conditions, Cl^- concentrations in groundwater within alluvial-proluvial fans generally remain below 100 mg/L (Huang et al. 2022). Groundwater exhibiting Cl^- concentrations exceeding 100 mg/L is likely impacted by anthropogenic influence. Samples with Cl^- concentrations exceeding 300 mg/L consistently have NH_4^+-N levels above 0.5 mg/L, primarily distributed in the upper right region of Fig. 3c. These samples are influenced by pollution from both chloride and ammonia nitro-

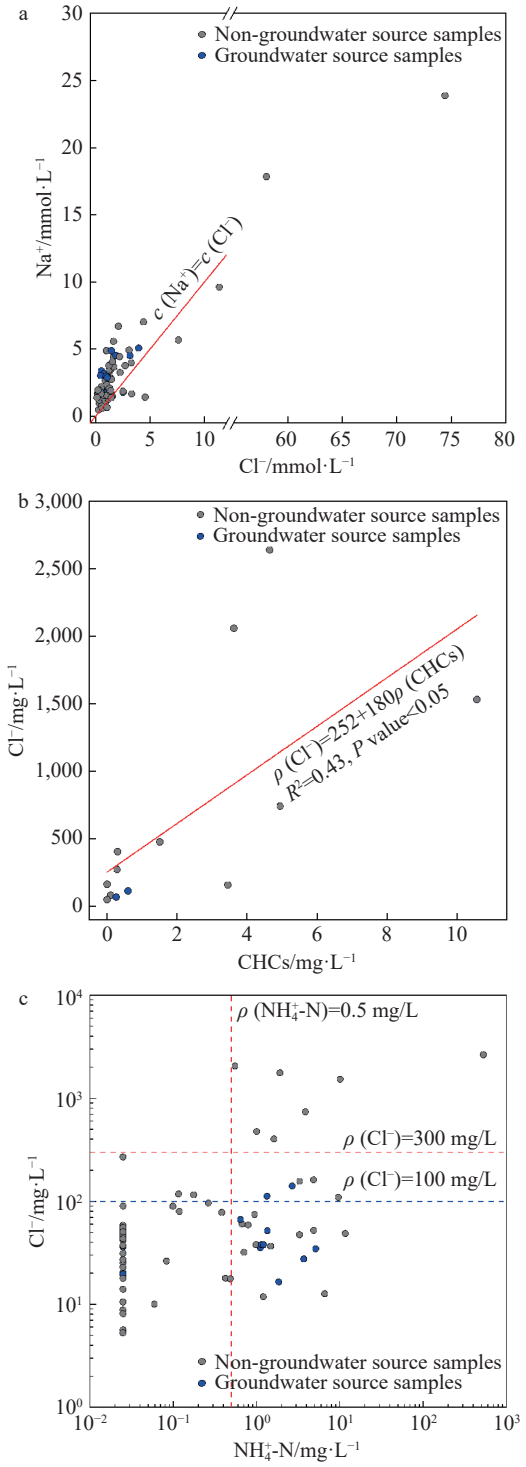

Fig. 3 Relationships of Na^+ vs. Cl^- (a), Cl^- vs. CHCs (b), and Cl^- vs. NH_4^+-N (c) for the analysis of factors controlling groundwater chemistry

gen. The presence of high NH_4^+ alongside low Cl^- concentrations serves as a key indicator of naturally occurring NH_4^+ within groundwater (Hinkle et al. 2007). Samples with NH_4^+-N > 0.5 mg/L and Cl^- < 100 mg/L are distributed in the lower right part of the figure, accounting for 25% of all samples and including 8 groundwater source wells. It is preliminarily inferred that high ammonia nitrogen levels in these samples are of geological origin. Overall, the concentrations of NH_4^+-N and Cl^- in the groundwater are influenced by both natural evolution and industrial activities.

3.2 NBLs evaluation

3.2.1 Pre-selection of original samples

In the HCA dendrogram of candidate pollution indicators (Fig. 4), NH_4^+-N, Cl^-, TDS, Ca^{2+}, Na^+, NO_3^--N, and CHCs were grouped together as the primary characteristic pollution indicators. In contrast, NO_2^--N, Fe, Mn, COD, and Cl/Br were categorized into a separate cluster. Given that Cl/Br is commonly used to indicate groundwater contamination from domestic wastewater (Panno et al. 2006; Katz et al. 2011; Pastén-Zapata et al. 2014; Linhoff, 2022), its separate grouping from NH_4^+-N implies a minimal association between NH_4^+-N in groundwater and domestic wastewater.

The correlation diagrams depicting characteristic pollution indicators for potential contamination sources, reservoir water, and groundwater (Fig. 5) positioned NH_4Cl waste liquid, calcium carbide slag samples, and water samples with NH_4^+-N concentrations above 0.5 mg/L and Cl^- concentrations exceeding 250 mg/L in the diagrams' upper right quadrant. These samples generally exhibited TDS greater than 1,000 mg/L, Na^+ concentrations over 100 mg/L, NO_3^--N concentrations above 2 mg/L, and Ca^{2+} concentrations exceeding 100 mg/L, suggesting potential contamination from NH_4Cl waste liquid and calcium carbide slags at these sites. Furthermore, the presence of CHCs in these water samples, typically associated with the recirculating cooling water from the PVC chemical plant, indicates possible contamination from

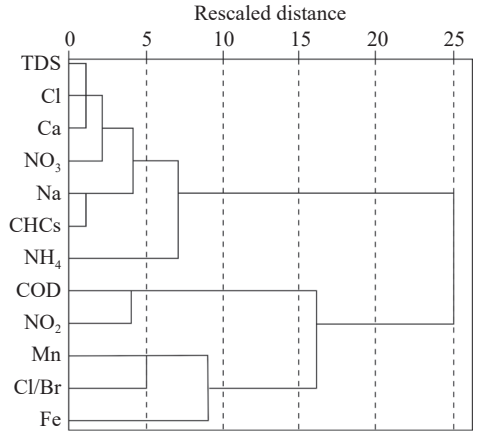

Fig. 4 The HCA-derived dendrogram for NH_4^+ and other characteristic pollution indicators

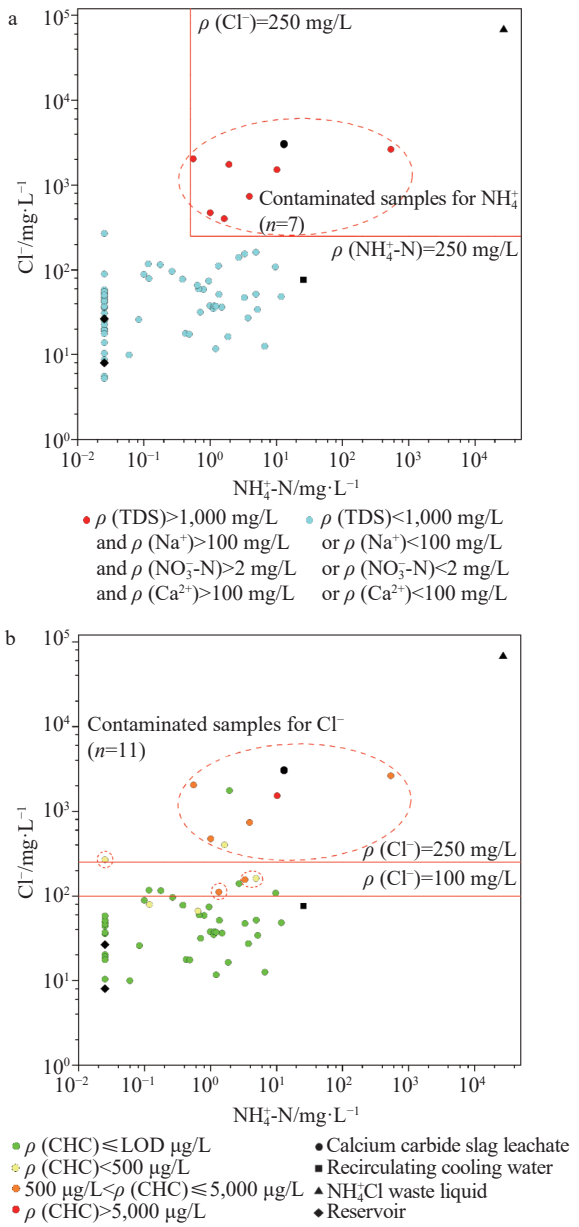

Fig. 5 Diagrams showing the relationships between NH_4^+, Cl^-, and other characteristic pollution indicators for uncontaminated surface water, potential contamination sources, and groundwater in the study area

Notes: The red lines in the diagrams denote the determination threshold for contamination. For samples below the detection limit, the detection limit value was taken as their ammonia nitrogen concentrations for plotting.

this source as well.

Despite the high ammonia nitrogen concentration (25.71 mg/L) found in the recirculating cooling water, its tendency to be adsorbed by aquifer sediments reduces its migration capacity (Domenico and Schwartz, 1998), thereby constraining the spread of contamination. Additionally, the recirculating cooling water exhibited low Cl^- concentrations, under 100 mg/L, indicating it is unlikely to be a major source of severe ammonia nitrogen and chloride contamination in the groundwater.

CHCs were detected in samples from six sites with NH_4^+-N concentrations below 0.5 mg/L or Cl^- concentrations under 250 mg/L, pointing to potential contamination from recirculating cooling water. Among these, four sites had Cl^- concentrations over 100 mg/L, suggesting possible influence from NH_4Cl waste liquid or calcium carbide slags as well.

In summary, NH_4^+-N > 0.5 mg/L and Cl^- > 250 mg/L were established as threshold criteria for identifying ammonia nitrogen pollution in groundwater. 7 samples exceeding these thresholds in the upper right region of the threshold line were classified as contaminated and removed from the original dataset. The remaining samples were labeled as the PS dataset, comprising 69 samples (Fig. 5a). For Cl^-, a threshold of > 250 mg/L and > 100 mg/L combined with detectable CHCs was used to identify contaminated samples, resulting in 11 samples classified as polluted, with the other 63 samples forming the PS dataset.

To validate the identified pollution samples, HCA was performed on groundwater samples using the characteristic pollution indicators (Fig. 6). Only samples with detectable ammonia nitrogen were included, as non-detection indicated no ammonia nitrogen pollution. The Within-Cluster Sum of Squares (WCSS) was calculated for different numbers of clusters to evaluate clustering performance. The optimal number of clusters was determined by plotting WCSS against the number of clusters (Fig. 6a), where a marked inflection point appeared at three clusters, indicating this as the optimal solution. Increasing the number of clusters beyond three resulted in minimal improvement in WCSS. As shown in Fig. 6b, the samples were divided into three clusters, with the 7 identified ammonia nitrogen pollution samples clustering into two groups, clearly separated from the uncontaminated samples. This demonstrates that the identification of contaminated samples was both effective and reasonable.

3.2.2 NBLs evaluation

Grubbs' test was applied to NH_4^+-N and Cl^- within the groundwater PS dataset of the study area. Since the detection rate of ammonia nitrogen was below 75%, all detected values were used for outlier detection. At a significance level of 0.05, the test identified two NH_4^+-N outliers and one Cl^- outlier (Fig. 7). The outliers were removed, resulting in NBLs datasets with 67 samples for NH_4^+-N and 62 samples for Cl^-, with maximum values of 6.6 mg/L

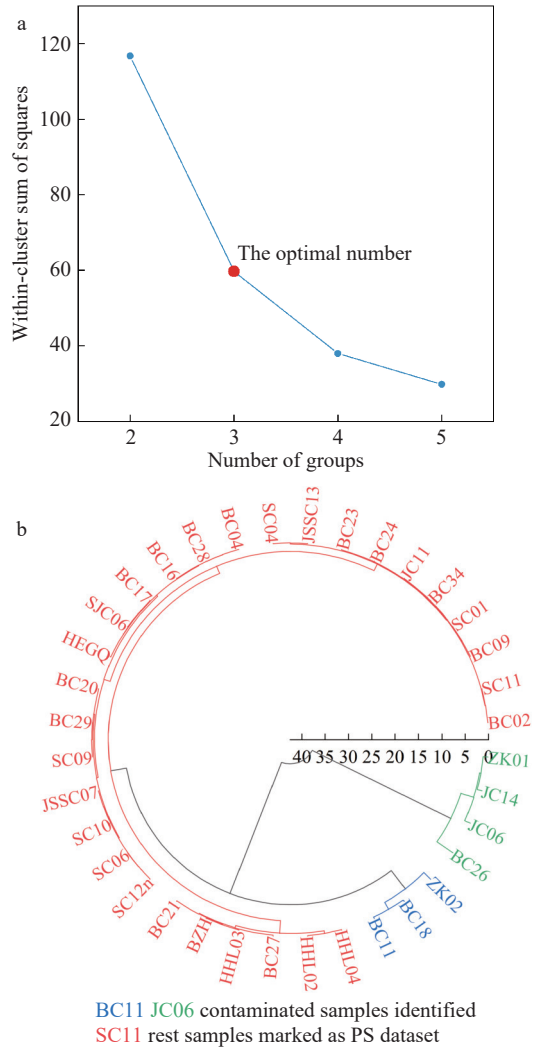

Fig. 6 HCA of groundwater samples

Note: (a) shows the selection of the optimal number of clusters, and (b) presents the clustering results, validating the identified contaminated samples.

and 118.0 mg/L, respectively. The Q-Q plot (Fig. S2) and Shapiro-Wilk test (Shapiro and Wilk, 1965) indicated that the NBLs dataset deviated from a normal distribution at the 0.05 significance level. Consequently, the 95th percentile was used to establish the NBLs, resulting in values of 5.2 mg/L for NH_4^+-N and 96.4 mg/L for Cl^-.

3.2.3 NBLs's effectiveness testing

The effectiveness of the NBLs assessment method in this study was evaluated by comparing the statistical parameters and tests of NH_4^+-N and Cl^- among the original dataset, the NBLs dataset, and the preindustrial dataset. The preindustrial dataset consists of groundwater quality data collected before industrial development in the study area, including 11 samples from the 1970s and 1980s. Their locations and detection results are shown in Fig. 1 and Table S4.

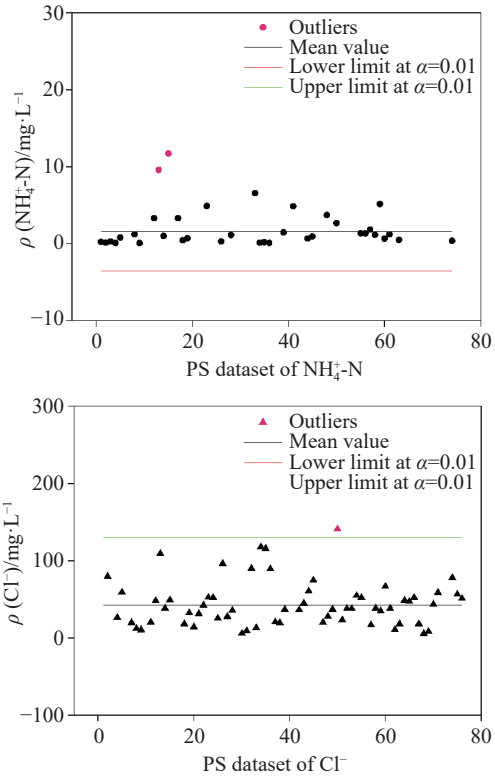

Fig. 7 NH_4^+-N and Cl^- outliers in the PS dataset, identified using Grubbs' test

The maximum values, standard deviations, skewness, and kurtosis of NH_4^+-N and Cl^- in the original dataset were much higher than those in the NBLs and preindustrial datasets (Table 2). The maximum concentrations of NH_4^+-N (5.4 mg/L) and Cl^- (75.9 mg/L) in the preindustrial dataset were comparable to the assessed NBLs, and the statistical parameters of this dataset were also similar to those of the NBLs dataset.

A one-sample t-test was conducted on the preindustrial dataset. At a significance level of 0.05, using the mean values of the original dataset (NH_4^+-N = 8.2 mg/L, Cl^- = 176.4 mg/L) as reference, the p-values for both parameters were less than 0.001. Using the mean values of the NBLs dataset (NH_4^+-N = 0.8 mg/L, Cl^- = 41.9 mg/L), the p-values exceeded 0.05. These results indicate that the preindustrial dataset differs significantly from the original dataset but is not significantly different from the NBLs dataset, suggesting that the NBLs dataset mainly reflects natural conditions with minimal human impact. These findings demonstrate that combining pre-selection with statistical methods for NBLs assessment is feasible and effective.

3.2.4 Factors controlling the NBLs of ammonia nitrogen

Groundwater naturally enriched in NH_4^+ has been

Table 2 Statistical characteristics of NH_4^+-N and Cl^- in groundwater of the study area based on the preindustrial, original, and NBLs datasets

Statistics	NH_4^+-N			Cl^-		
	Original dataset	NBLs dataset	Preindustrial dataset	Original dataset	NBLs dataset	Preindustrial dataset
Sample size	76	67	11	74	62	11
Max. (mg/L)	529.32	**6.6**	5.4	2641	**118.0**	75.9
Med. (mg/L)	0.2	0.06	0.05	43.8	37.3	20.6
Mean (mg/L)	8.2	0.8	0.96	176.4	41.9	28.1
St. Dev. (mg/L)	60.6	1.4	1.89	462.3	27.4	23.8
Skewness	8.7	2.4	2	4.0	1	1.7
Kurtosis	75.8	5.4	2.9	16.2	0.8	1.5
One-sample t-test (P value)	<0.001	0.79	/	<0.001	0.08	/

documented across diverse global locations, including Vietnam's Red River Delta (Berg et al. 2001), northern Mexico (Ortega-Guerrero, 2003), Oregon and eastern Illinois in the U.S. (Hinkle et al. 2007; Glessner and Roy, 2009), Italy's Po River Delta (Mastrocicco et al. 2013), and China's Songnen Plain (Lin, 2000), Jianghan Plain (Du et al. 2017), and Pearl River Delta (Jiao et al. 2010). Studies suggest that such high NH_4^+ concentrations in groundwater predominantly arise from the mineralization and hydrolysis of nitrogenous organic matter, often linked to the organic content within geological layers. The amount of nitrogenous organic matter present is a key determinant of NH_4^+ 's NBLs in groundwater (Böhlke et al. 2006; Mooshammer et al. 2014; Du Y et al. 2017; Huang et al. 2022). Nitrogen isotope analyses for the study area revealed that the ^{15}N concentration in exchangeable ammonium in natural sediments aligns with organic nitrogen ^{15}N concentrations in natural sediments from other areas (Liu et al. 2023), indicating that organic-rich sediments significantly contribute to the naturally elevated NH_4^+-N concentrations in groundwater in the study area, thereby influencing NH_4^+-N's NBLs.

3.2.5 Factors controlling the NBLs of Cl

Natural Cl sources of groundwater include dissolution of minerals in ancient seawater, halite, and evaporites within sediments (Belkhiri et al. 2012). In the Hohhot Basin, the groundwater's chemical composition is largely shaped by halite dissolution, alongside cation exchange and adsorption processes (Dong et al. 2022). The basin's history of multiple lake surface expansions since the Late Pleistocene has led to the deposition of several layers of lacustrine sediments in the shallow aquifer, enriching it with water-soluble salts (Dong et al. 2022). Consequently, the NBLs of Cl in groundwater of the study area are somewhat elevated when compared to other alluvial-proluvial regions in China, such as the eastern Hohhot Basin (Li et al. 2020), Pearl River Delta (Huang et al. 2022), and Qinling Mountains (Gao et al. 2020). This elevated NBLs is uncommon in alluvial fans of arid and semi-arid regions. Although evaporation rates are much higher than in the Pearl River Delta, the study area is situated on a piedmont alluvial fan with deep groundwater tables, so evaporation has a limited influence on groundwater chemistry. The primary cause of this difference is the region's distinctive geological structure and depositional history.

3.3 Contamination evaluation

3.3.1 Contamination degree

Contaminated zones were identified using the detected contaminated samples, with corresponding pollution indices computed. The ammonia nitrogen contamination was predominantly located in the industrial park's south-central zone. Two samples, proximal to the NH_4Cl waste liquid and calcium carbide slags, had pollution indices of 1,048.2 and 9.8, respectively, pinpointing a source area of severe groundwater contamination. Meanwhile, the larger chloride contamination zone spanned the industrial park's south-central zone and extended into the northern water source area, with pollution indices ranging from 0.1 to 10.2. The highest values were noted near the contamination sources, diminishing outward, indicating a decrease in the contamination degree. In the northern water source wells, values did not surpass 0.2, reflecting only mild contamination (Fig. 8).

However, using pollution indices to gauge groundwater contamination degree has its drawbacks. Due to the spatial variability of NBLs, a singular NBLs-derived pollution index may not

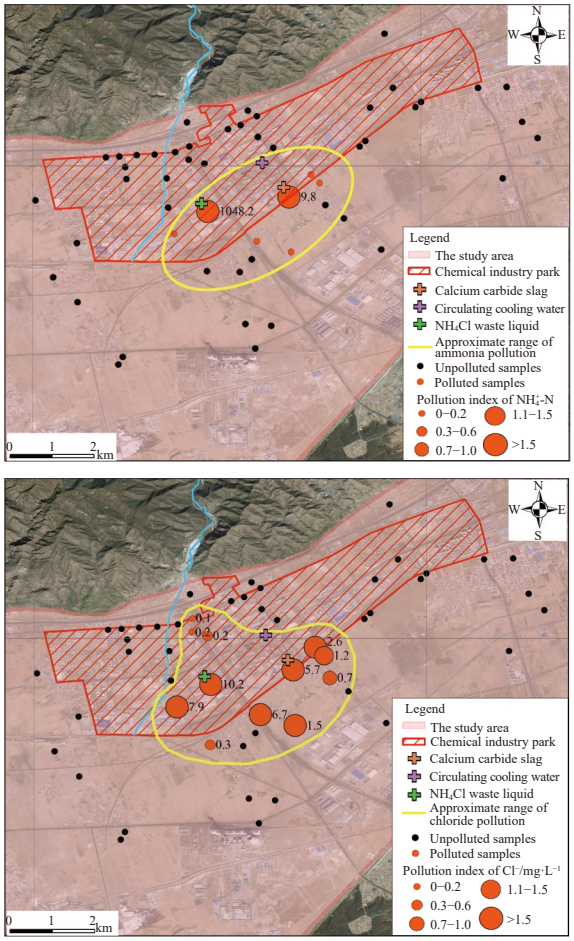

Fig. 8 Distributions, pollution indices, and preliminarily delineated contaminated zones of NH_4^+-N- and Cl^--contaminated samples

fully or accurately represent each sample's contamination degree. For example, in this study, employing the 95% quantile as the NBLs might lead to an underestimation of the actual contamination degree (Zanotti et al. 2022). Ideally, spatially continuous NBLs should be derived through interpolation (Dalla et al. 2017; Molinari et al. 2019; Zanotti et al. 2022). In this study, we did not perform interpolation because the NBLs dataset cannot reliably meet the accuracy requirements for predicting data density (Li and Heap, 2014). This is due to the contamination samples being concentrated over a relatively large area and the absence of historical groundwater data in that region, which raises questions about whether the predicted values can accurately reflect the true background levels under these conditions. Despite these limitations, pollution indices are useful for management purposes, offering preliminary insights into potential contamination and its degree in newly collected samples, thus aiding in decision-making for survey expansion or remediation planning.

3.3.2 Management recommendations

This study concludes that ammonia nitrogen concentrations in the northern water source wells of the industrial park fall within the expected NBLs range, indicating an absence of contamination influence. Chloride contamination, however, warrants more attention due to its potential for adverse effects. The extensive use of the water source area has disrupted the natural groundwater flow, causing chloride from the heavily contaminated zone in the southern part of the industrial park to migrate northward, leading to slight contamination in some water source wells. Consequently, contamination control efforts should not be confined to the park's southern zone but should also focus on the norther zones. Further studies and numerical simulations are essential to forecast the spread and diffusion of chloride under various extraction scenarios and to precisely map out the contaminated groundwater zones for the formulation of effective remediation strategies.

4 Conclusion

This study employed an improved pre-selection method to estimate the groundwater NBLs of ammonia nitrogen and chlorides in the alluvial fan of Tuzuoqi, Hohhot, Inner Mongolia. The method enabled assessment of the spatial extent and severity of pollution. HCA identified NH_4^+, Cl^-, TDS, Ca^{2+}, Na^+, NO_3^-, and CHCs as characteristic pollution indicators for the area. The pollution thresholds were set as follows: NH_4^+-N > 0.5 mg/L combined with Cl^- > 250 mg/L for ammonia nitrogen, Cl^- > 250 mg/L and Cl^- > 100 mg/L with simultaneous detection of CHCs for chloride. Using these criteria, seven samples with ammonia nitrogen pollution and eleven samples with chloride pollution were excluded from the original dataset, resulting in the PS dataset. After applying Grubbs' test and normality assessments, the PS dataset was used to derive the NBLs dataset. The results of the single-sample t-test indicate no significant difference between the NBLs dataset and historical data. This suggests that the improved pre-selection method used in this study is effective for determining the NBLs of groundwater in the study area, which is representative of the local industrial pollution region.

A unified NBLs was used to calculate the pollution index and assess groundwater contamination. The unified NBLs value was set at the 95th percentile of the NBLs dataset, as the dataset does not follow a normal distribution. While this

approach simplifies the assessment, it does not fully account for the heterogeneity of hydrogeological conditions across the study area, potentially leading to deviations from actual pollution levels. This decision was made because the spatial distribution of pollution samples is extensive, and the region lacks sufficient historical monitoring data, making it difficult to ensure accurate interpolation of the NBLs dataset. Future studies could explore alternative interpolation methods, such as probabilistic kriging, to better capture the heterogeneity of the geological conditions. Such methods could also estimate the probability and uncertainty of concentrations exceeding the NBLs, providing a more comprehensive understanding.

The pollution index reveals that ammonia nitrogen pollution is relatively localized, mainly concentrated in the southeastern industrial park and areas near pollution sources. Groundwater from water supply wells shows no signs of ammonia nitrogen contamination, with maximum values below the NBLs dataset, well within national Class III water quality standards. The elevated background levels are attributed to natural geological factors, specifically organic-rich lacustrine deposits, as discussed in related studies. The chloride pollution area is broader, extending from the southeastern to the northern parts of the industrial park, causing slight contamination in some water sources. Compared to other alluvial fans, the relatively high background levels of chloride are linked to the high water-soluble salt content in lacustrine sediments within the strata. Based on these findings, it is recommended to implement routine monitoring of ammonia nitrogen and chloride in the industrial park, establish reasonable pollution control targets, and prioritize realistic management goals without overestimating water quality improvement efforts.

Acknowledgements

This research was supported by the National Key Research and Development Program (2019YFC0409200).

References

Ahmadi S, Jahanshahi R, Moeini V, et al. 2018. Assessment of hydrochemistry and heavy metals pollution in the groundwater of Ardestan mineral exploration area, Iran. Environmental Earth Sciences, 77: 1−13. DOI：10.1007/s12665-018-7393-7.

Allia Z, Lalaoui M. 2024. Formation mechanism of hydrochemical and quality evaluation of shallow groundwater in the Upper Kebir subbasin, Northeast Algeria. Journal of Groundwater Science and Engineering, 12(1): 78−91. DOI：10.26599/JGSE.2024.9280007.

Analytical Methods Committee AN. 2015. Using the Grubbs and Cochran tests to identify outliers. Analytical Methods, 7(19): 7795−7948. DOI：10.1039/c5ay90053k.

Belkhiri L, Mouni L, Boudoukha A. 2012. Geochemical evolution of groundwater in an alluvial aquifer: Case of El Eulma aquifer, East Algeria. Journal of African Earth Sciences, 66-67: 46−55. DOI：10.1016/j.jafrearsci.2012.03.001.

Berg M, Tran HC, Nguyen TC, et al. 2001. Arsenic contamination of groundwater and drinking water in vietnam: A human health threat. Environmental Science and Technology, 35(13): 2621−2626. DOI：10.1021/es010027y.

Bi P, Huang GX, Liu CY, et al. 2022. Geochemical factors controlling natural background levels of phosphate in various groundwater units in a large-scale urbanized area. Journal of Hydrology, 608: 127594. DOI: 10.1016/j.jhydrol.2022.127594.

Biddau R, Cidu R, Lorrai M, et al. 2017. Assessing background values of chloride, sulfate and fluoride in groundwater: A geochemical-statistical approach at a regional scale. Jounal of Geochemical Exploration, 181: 243−255. DOI：10.1016/j.gexplo.2017.08.002.

Böhlke JK, Smith RL, Miller DN. 2006. Ammonium transport and reaction in contaminated groundwater: Application of isotope tracers and isotope fractionation studies. Water Resources Research, 42: W05411. DOI: 10.1029/2005WR004349.

Bondu R, Humez P, Mayer B, et al. 2022. Estimating natural background concentrations for dissolved constituents in groundwater: A methodological review and case studies for geogenic fluoride. Journal of Geochemical Exploration, 233: 106906. DOI: 10.1016/j.gexplo.2021.106906.

Bulut OF, Duru B, Cakmak O, et al. 2020. Determination of groundwater threshold values: A methodological approach. Journal of Cleaner

Production, 253: 120001. DOI: 10.1016/j.jclepro.2020.120001.

Chen K, Liu QM, Peng WH, et al. 2022. Source apportionment and natural background levels of major ions in shallow groundwater using multivariate statistical method: A case study in Huaibei Plain, China. Journal of Environmental Management, 301: 113806. DOI:10.1016/j.jenvman.2021.113806.

Dalla LN, Fabbri P, Mason L, et al. 2017. Geostatistics as a tool to improve the natural background level definition: An application in groundwater. Science of the Total Environment, 598: 330−340. DOI：10.1016/j.scitotenv.2017.04.018.

Davis SN, Whittemore DO, Fabryka-Martin J. 1998. Uses of chloride/bromide ratios in studies of potable water. Ground water, 36(2): 338−350. DOI：10.1111/j.1745-6584.1998.tb01099.x.

De Caro M, Crosta GB, Frattini P. 2017. Hydrogeochemical characterization and natural background levels in urbanized areas: Milan metropolitan area (northern Italy). Journal of Hydrology, 547: 455−473. DOI：10.1016/j.jhydrol.2017.02.025.

Domenico, PA, Schwartz FW. 1998. Physical and chemical hydrogeology, second edition. John Wiley & Sons, Inc, New York.

Dong S, Liu B, Chen Y, et al. 2022. Hydrogeochemical control of high arsenic and fluoride groundwater in arid and semi-arid areas: A case study of Tumochuan Plain, China. Chemosphere. 301: 134657. DOI: 10.1016/j.chemosphere.2022.134657.

Du Y, Ma T, Deng Y, et al. 2017. Sources and fate of high levels of ammonium in surface water and shallow groundwater of the Jianghan plain, Central China. Environmental Science: Process Impacts, 19(2): 161−172. DOI：10.1039/c6em00531d.

Ducci D, de Melo M, Preziosi E, et al. 2016. Combining natural background levels (NBLs) assessment with indicator kriging analysis to improve groundwater quality data interpretation and management. Science of the Total Environment, 569-570: 569−584. DOI：10.1016/j.scitotenv.2016.06.184.

European Community. 2006. Groundwater directive 2006/118/CE. Directive of the European Parliament and of the Council on the Protection of Groundwater Against Pollution and Deterioration, OJ L372, 27/12/2006, 19–31.

Gao Y, Qian H, Huo C, et al. 2020. Assessing natural background levels in shallow groundwater in a large semiarid drainage basin. Journal of Hydrology, 584: 124638. DOI：10.1016/j.jhydrol.2020.124638.

General Administration of Quality Supervision (GAQS). 2017. Inspection and Quarantine of the People's Republic of China (IQPRC). Standard for groundwater quality. GB/T 14848-2017, ICS: 13.060, Z: 50.

Glessner JJG, Roy WR. 2009. Paleosols in central illinois as potential sources of ammonium in groundwater. Ground water Monitoring and Remediation, 29(4): 56−64. DOI：10.1111/j.1745-6592.2009.01257.x.

Guo GX, Xin BD, Liu WC, et al. 2010. Review on the study of the environment background values of groundwater in China. Hydrogeology and Engineering Geology, 37(2): 95−98. (in Chinese) DOI：10.3969/j.issn.1000-3665.2010.02.021.

He BN, He JT, Sun JC, et al. 2022. Comprehensive evaluation of regional groundwater pollution: Research status and suggestions. Earth Science Frontiers, 29(3): 51−63. (in Chinese) DOI：10.13745/j.esf.sf.2022.1.29.

Hinkle SR, Bohlke JK, Duff JH, et al. 2007. Aquifer-scale controls on the distribution of nitrate and ammonium in ground water near La Pine, Oregon, USA. Journal of Hydrology, 333(2-4): 486−503. DOI：10.1016/j.jhydrol.2006.09.013.

Hinsby K, Condesso DMM, Dahl M. 2008. European case studies supporting the derivation of natural background levels and groundwater threshold values for the protection of dependent ecosystems and human health. Science of the Total Environment, 401: 1−20. DOI：10.1016/j.scitotenv.2008.03.018.

Huang GX, Pei LX, Li LP, et al. 2022. Natural background levels in groundwater in the Pearl River Delta after the rapid expansion of urbanization: A new pre-selection method. Science of the Total Environment, 813: 151890. DOI：10.1016/j.scitotenv.2021.151890.

Jiao JJ, Wang Y, Cherry JA, et al. 2010. Abnor-

mally high ammonium of natural origin in a coastal aquifer-aquitard system in the Pearl River Delta, China. Environmental Science and Technology, 44(19): 7470−7475. DOI：10.1021/es1021697.

Katz BG, Eberts SM, Kauffman LJ. 2011. Using Cl/Br ratios and other indicators to assess potential impacts on groundwater quality from septic systems: A review and examples from principal aquifers in the united states. Journal of Hydrology, 397(3): 151−166. DOI：10.1016/j.jhydrol.2010.11.017.

Khadra WM, Elias AR, Majdalani MA. 2022. A systematic approach to derive natural background levels in groundwater: Application to an aquifer in North Lebanon perturbed by various pollution sources. Science of the Total Environment, 847: 157586. DOI：10.1016/j.scitotenv.2022.157586.

Lan FN, Zhao Y, Li J, et al. 2024. Health risk assessment of heavy metal pollution in groundwater of a karst basin, SW China. Journal of Groundwater Science and Engineering, 12(1): 49−61. DOI：10.26599/JGSE.2024.9280005.

Li J, Heap AD. 2014. Spatial interpolation methods applied in the environmental sciences: A review. Environmental Modelling and Software, 53: 173−189. DOI：10.1016/j.envsoft.2013.12.008.

Li XY, Zhang YL, Wang LJ, et al. 2020. Study on groundwater environmental background values in Hetao Basin. Journal of Arid Land Resources and Environment, 34(3): 180−187. (in Chinese) DOI：10.13448/j.cnki.jalre.2020.83.

Lin XY, Chen MX, Wang ZX, et al. 2000. Research on groundwater resources and sustainable development in Songnen basin. Seismological Press, Beijing.

Linhoff B. 2022. Deciphering natural and anthropogenic nitrate and recharge sources in arid region groundwater. Science of the Total Environment, 848: 157345. DOI：10.1016/j.scitotenv.2022.157345.

Liu JY, Yuan JL, Zhang YL, et al. 2023. Identification of ammonium source for groundwater in the piedmont zone with strong runoff of the Hohhot Basin based on nitrogen isotope. Science of the Total Environment, 882: 163650. DOI：10.1016/j.scitotenv.2023.163650.

Lu L, Li W, Cheng Y, et al. 2023. Chemical recycling technologies for PVC waste and PVC-containing plastic waste: A review. Waste Management, 166: 245−258. DOI：10.1016/j.wasman.2023.05.012.

Magaritz M, Nadler A, Koyumdjisky H, et al. 1981. The use of Na/Cl ratios to trace solute sources in a semiarid zone. Water Resources Research, 17: 602−608. DOI：10.1029/wr017i003p00602.

Mastrocicco M, Giambastiani B, Colombani N. 2013. Ammonium occurrence in a salinized lowland coastal aquifer (Ferrara, Italy). Hydrological Process, 27(24): 3495−3501. DOI：10.1002/hyp.9467.

Ministry of Ecological Environment of China (MEEC). 2021. Technical plan for investigation and evaluation of groundwater environment in chemical industrial parks. Ministry of Ecological Environment of China, Beijing. (in Chinese)

Molinari A, Guadagnini L, Marcaccio M, et al. 2012. Natural background levels and threshold values of chemical species in three large-scale groundwater bodies in northern Italy. Science of the Total Environmental, 425(15): 9−19. DOI：10.1016/j.scitotenv.2012.03.015.

Molinari A, Guadagnini L, Marcaccio M, et al. 2019. Geostatistical multimodel approach for the assessment of the spatial distribution of natural background concentrations in large-scale groundwater bodies. Water Research, 149: 522−532. DOI：10.1016/j.watres.2018.09.049.

Mooshammer M, Wanek W, Hammerle I, et al. 2014. Adjustment of microbial nitrogen use efficiency to carbon: Nitrogen imbalances regulates soil nitrogen cycling. Nature Communications, 5: 3694. DOI：10.1038/ncomms4694.

Nisi B, Buccianti A, Raco B, et al. 2016. Analysis of complex regional databases and their support in the identification of background/baseline compositional facies in groundwater investigation: Developments and application examples. Journal of Geochemical Exploration, 164: 3−17. DOI：10.1016/j.gexplo.2015.06.019.

Ortega-Guerrero A. 2003. Origin and geochemical evolution of groundwater in a closed-basin clayey aquitard, Northern Mexico. Journal of Hydrology, 284(1): 26−44. DOI：10.1016/S0022-1694(03)00239-7.

Panno SV, Hackley KC, Hwang HH, et al. 2006. Characterization and identification of Na-Cl sources in ground water. Ground Water, 44(2): 176−187. DOI：10.1111/j.1745-6584.2005.00127.x.

Panno SV, Kelly WR, Martinsek AT, et al. 2006. Estimating background and threshold nitrate concentrations using probability graphs. Ground Water, 44(5): 697−709. DOI：10.1111/j.1745-6584.2006.00240.x.

Parrone D, Ghergo S, Preziosi E. 2019. A multi-method approach for the assessment of natural background levels in groundwater. Science of the Total Environment, 659: 884−894. DOI：10.1016/j.scitotenv.2018.12.350.

Pastén-Zapata E, Ledesma-Ruiz R, Harter T, et al. 2014. Assessment of sources and fate of nitrate in shallow groundwater of an agricultural area by using a multi-tracer approach. Science of the Total Environment, 470-471: 855−864. DOI：10.1016/j.scitotenv.2013.10.043.

Reimann C, Garrett RG. 2005. Geochemical background—concept and reality. Science of the Total Environment, 350(1): 12−27. DOI：10.1016/j.scitotenv.2005.01.047.

Serianz L, Cerar S, Sraj M. 2020. Hydrogeochemical characterization and determination of natural background levels (NBLs) in groundwater within the main lithological units in slovenia. Environment Earth Science, 79(15): 373. DOI：10.1007/s12665-020-09112-1.

Shapiro SS, Wilk MB. 1965. An analysis of variance test for normality (complete samples). Biometrika, 52(3/4): 591−611.

Wendland F, Berthold G, Blum A, et al. 2008. Derivation of natural background levels and threshold values for groundwater bodies in the Upper Rhine Valley (France, Switzerland and Germany). Desalination, 226: 160−168. DOI：10.1016/j.desal.2007.01.240.

Xiao J, Zhang F, Jin ZD. 2016. Spatial characteristics and controlling factors of chemical weathering of loess in the dry season in the middle Loess Plateau, China. Hydrological Process, 30: 4855−4869. (in Chinese) DOI：10.1002/hyp.10959.

Xiong Y, Du Y, Deng Y, et al. 2022. Feammox in alluvial-lacustrine aquifer system: Nitrogen/iron isotopic and biogeochemical evidences. Water Research, 222: 118867. DOI：10.1016/j.watres.2022.118867.

Zanotti C, Caschetto M, Bonomi T, et al. 2022. Linking local natural background levels in groundwater to their generating hydrogeochemical processes in Quaternary alluvial aquifers. Science of the Total Environment, 805: 150259. DOI：10.1016/j.scitotenv.2021.150259.

Zhang ZP, Zhu YC, Hao QC, et al. 2017. A study on variation mechanism of groundwater flow system in the Hohhot basin and its resources effect analysis. Hydrogeology and Engineering Geology, 44(2): 63−68. (in Chinese) DOI：10.16030/j.cnki.issn.1000-3665.2017.02.10.

Zhang J, Mei N, Liu MH, et al. 2020. Low temperature ammonia nitrogen removal from an iron, manganese, and ammonia groundwater purification process with different concentrations of iron and manganese. Environmental Science, 41(6): 2727−2735. (in Chinese) DOI：10.13227/j.hjkx.201912111.

Zhou NQ, Liu KH, Guo MS, et al. 2025. Analysis of spatiotemporal evolution characteristics and driving factors of carbon storage in Dongting Lake Wetland, China. Journal of Groundwater Science and Engineering, 13(2): 156−169. DOI：10.26599/JGSE.2025.9280046.